MATHEMATICA APPLICANDA
Vol. 50(1) 2022, p. 107–128
doi: 10.14708/ma.v50i1.7151

Pitágoras Pinheiro de Carvalho (Teresina)
Isaías Pereira de Jesus (Teresina)
Olimpio Pereira de Sá Neto (Parnaíba)

On the Computation of Hierarchical Control results for One-Dimensional Transmission Line

Abstract In this paper, motivated by a physics problem, we investigate some numerical and computational aspects of the problem of hierarchical controllability in one-dimensional wave equations in domains with a moving boundary. Some controls act in part of the boundary and define a strategy of equilibrium between them, considering a leader's control and a follower's. Thus, we introduced the concept of hierarchical control to solve the problem and mapped the Stackelberg Strategy between these controls. The numerical methods described here consist of a combination of the following: finite element method (FEM) for space approximation; finite difference method (FDM) for time discretization and fixed-point algorithm for the solution of the total discrete control problem. Data programming and computer simulations are performed in FreeFem++ and for a better presentation of the experiments we use Matlab.

2020 Mathematics Subject Classification: Primary: 93B05; Secondary: 93C05, 93C25, 65N06..

Key words and phrases: Controllability; Stackelberg strategy; Transmission line equation; Numerical Simulation..

1. Introduction

On several occasions, controlling a problem may involve more than one agent (control). For such situations, we can define a strategy that indicates the desired behavior. This paper deals with the numerical solution of a controllability problem for the wave equation through a hierarchy of controls in the boundary. More precisely, we have chosen the so-called *Stackelberg-Nash* method, which can be briefly described as follows:

- We have control of two kinds: leaders and followers.
- We associate to leader a *Nash* equilibrium, that corresponds to a non-cooperative multiple-objective optimal control problem.
- Then, we choose the leader among the set of controls by minimizing a suitable functional.

Initially, in game theory, a player is a strategic decision-maker within the context of the game. And the game is characterized by any set of circumstances that have an outcome depending on the actions of two or more decision-makers (players). In a hierarchical game, that is, in which all players make their decisions based on a decision by a leading player, and a result is achieved for all players, this is called the equilibria position. In our case, there will be no cooperation in decision-making between players. In other words, fixed a leader we will dedicate ourselves to the study of equilibria where there is a leader and the other players adopt Nash equilibrium in the equations. The process in the problems above is a combination of strategies and is called the Stackelberg-Nash strategy. For more details on the noncooperative optimization strategy proposed by Nash (see [26]) and the Stackelberg hierarchical-cooperative strategy (see [33]).

Some numerical and computational results involving *Nash* equilibrium we can found in [2], [29] and [30], the *Stackelberg-Nash* equilibrium in [7]. For the algorithm construction, we adapt the ideas contained in [8] in that the authors work in numerical viewpoint the *Nash equilibrium* for the wave equations, but the controls domains acting in subregions of the domain.

The main contribution of this article resides in the numerical results and computational simulations associated with hierarchical control problems in which the boundary conditions are moving.

The structure of the article is given as follows: In Section 2 we present a physical motivation for the problem. In Section 3 we give the problem formulation. Section 4 is devoted to studying the optimality systems for the leader and follower controls where the principal results for the strategy of *Nash* for the linear system are obtained as in [10]. Section 5 we leave it reserved for full discretization and presentation of the algorithm used to solve the problem. Section 6 and Appendices concentrates tables and numerical experiments resulting from the data simulation presented in Section 5. Finally, in Section 7 some comments and possible advances are added.

2. Physical Systems

When we transmit a microwave signal through a l length transmission line, if the wavelength is much greater than the cross-sectional dimension of the line, the loads on the transmission line can be considered as if they were moving in a single dimension, figure 1. The n radiation modes behaved in this transmission line can be modeled by a set of discrete and infinitesimal LC elements known as concentrated circuit elements *(lumped circuit)* [27, 14, 13, 15, 16, 12].

The Lagrangean in the system is:

$$\mathcal{L} = \sum_n \left[\frac{l i_n^2}{2} - \frac{q_n^2}{2c} \right], \tag{1}$$

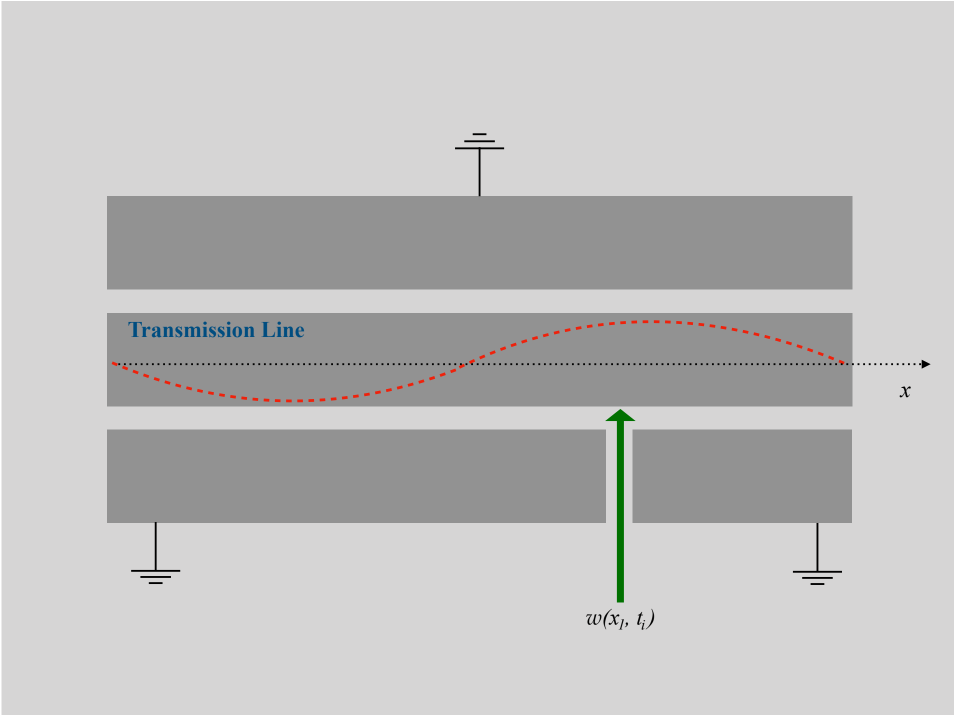

Figure 1: Modes of load density vibrations in a transmission line in the schematic model for spatially located control in time did not continue.

where c is the capacitance and l is the auto inductance of n - this is the mode of the transmission line. In this case, the temporal variation of the load at the n node of the circuit is given by $\dot{q_n} = i_{n-1} - i_n$ and $i_n = -\sum_{m=1}^{n} \dot{q_m}$ is the current at the node. Substituting in Lagrangean (1), we have

$$\mathcal{L} = \sum_n \left[\frac{l(\sum_{m=1}^{n} \dot{q}_m)^2}{2} - \frac{q_n^2}{2c} \right]. \tag{2}$$

As usual in this type of system we will make use of the infinitesimal nature of these elements (the degrees of freedom of the system) to take the equation (2) into the continuum. We define the variable

$$u(x,t) = \int_{-\frac{L}{2}}^{x} dx^{'} q(x^{'}, t) \tag{3}$$

where $q(x)$ is the linear density of charge. Making the substitutions:

$$\sum_n^{m=1} q_m(t) \to u(x,t), \qquad q_n(t) \to q(x,t) = \frac{\partial u}{\partial x},$$

one-dimensional Lagrangean density is written

$$\mathcal{L} = \frac{l\dot{u}^2}{2} - \frac{1}{2c}\left[\frac{\partial u}{\partial x}\right]^2. \tag{4}$$

Here c and l are transformed into linear capacitance density and transmission line inductance, respectively. Applying Euler-Lagrange to (4), we obtain

$$\frac{1}{c}\frac{\partial^2 u}{\partial x^2} - l\frac{\partial^2 u}{\partial t^2} = 0, \tag{5}$$

where $1/\sqrt{lc}$ is the velocity of the wave propagation. For our present problem, we will consider the wave equation with dimensionless velocity $1/\sqrt{lc} = 1$, and simplifications of annotations for

$$\frac{\partial^2 u}{\partial x^2} \equiv u_{xx},$$

and

$$\frac{\partial^2 u}{\partial t^2} \equiv u_{tt}.$$

3. Statement of the problem

The research about controllability of the wave equation has been the subject of study by many authors in the last years. We encourage the reading of the surveys due to Cui et al. [4]. In this article we study the controllability of this equation by the view of a multiobjective problem.

More precisely, let $T > 0$. Given $k \in (0,1)$, set $\alpha_k(t) = 1+kt$, for $t \in (0,T)$. Let us consider the non-cylindrical domain constructed as in [10] given by:

$$\widehat{Q} = \left\{(x,t) \in \mathbb{R}^2;\ 0 < x < \alpha_k(t),\ \ t \in (0,T)\right\},$$

with lateral boundary defined by $\widehat{\Sigma} = \widehat{\Sigma}_0 \cup \widehat{\Sigma}_0^*$, where

$$\widehat{\Sigma}_0 = \{(0,t);\ t \in (0,T)\} \quad \text{and} \quad \widehat{\Sigma}_0^* = \widehat{\Sigma}\backslash\widehat{\Sigma}_0 = \{(\alpha_k(t),t);\ t \in (0,T)\}.$$

Note that the domain grows linearly in time (function alpha). We denote by Ω_t and Ω_0 the intervals $(0,\alpha_k(t))$ and $(0,1)$ respectively, and consider the controlled string equation in the domain $\widehat{Q}$:

$$\begin{cases} u_{tt} - u_{xx} = 0 \quad \text{in} \quad \widehat{Q}, \\ u(x,t)\Big|_{\widehat{\Sigma}_0} = \widetilde{w}(t) \ \text{ and } \ u(x,t)\Big|_{\widehat{\Sigma}_0^*} = 0, \\ u(x,0) = u_0(x),\ \ u_t(x,0) = u_1(x) \ \text{ in } \ \Omega_0, \end{cases} \tag{6}$$

with u the state, $\widetilde{w}$ is the control, and $(u_0(x), u_1(x)) \in L^2(\Omega_0) \times H^{-1}(\Omega_0)$ are initial data.

From the physics point of view, Equation (6) represents the motion of a string where an endpoint is fixed and the other one is moving and the constant k is called the speed of the moving endpoint.

We consider

$$\widehat{\Sigma}_0 = \widehat{\Sigma}_1 \cup \widehat{\Sigma}_2, \tag{7}$$

and

$$\widetilde{w} = \{\widetilde{w}_1, \widetilde{w}_2\}, \quad \widetilde{w}_i = \text{control function in } \; L^2(\widehat{\Sigma}_i), \; i = 1, 2. \tag{8}$$

We can also write

$$\widetilde{w} = \widetilde{w}_1 + \widetilde{w}_2, \quad \text{with } \; \widehat{\Sigma}_0 = \widehat{\Sigma}_1 = \widehat{\Sigma}_2, \tag{9}$$

so that system (6) can be rewritten as follows:

$$\begin{cases} u_{tt} - u_{xx} = 0 \quad \text{in} \quad \widehat{Q}, \\ u(x,t)\Big|_{\widehat{\Sigma}_1} = \widetilde{w}_1(t), \quad u(x,t)\Big|_{\widehat{\Sigma}_2} = \widetilde{w}_2(t) \quad \text{and} \quad u(x,t)\Big|_{\widehat{\Sigma}\backslash\widehat{\Sigma}_0} = 0, \\ u(x,0) = u_0(x), \;\; u_t(x,0) = u_1(x) \;\; \text{in} \;\; \Omega_0. \end{cases} \tag{10}$$

Let us consider $\widetilde{w}_1$ as being the "main" control (the leader), $\widetilde{w}_2$ as the follower, in *Stackelberg* terminology and $u = u(x,t)$ the solution of (10). We will also introduce the *secondary* cost functional

$$\widetilde{J}_2(\widetilde{w}_1, \widetilde{w}_2) = \frac{1}{2} \iint_{\widehat{Q}} (u(\widetilde{w}_1, \widetilde{w}_2) - u_2)^2 \, dx \, dt + \frac{\sigma}{2} \int_{\widehat{\Sigma}_2} \widetilde{w}_2^2 \, d\widehat{\Sigma}, \tag{11}$$

and the *main* cost functional

$$\widetilde{J}(\widetilde{w}_1) = \frac{1}{2} \int_{\widehat{\Sigma}_1} \widetilde{w}_1^2 \, d\widehat{\Sigma}, \tag{12}$$

where σ is a positive constant and u_2 is a given function in $L^2(\widehat{Q})$.

By Milla Miranda [25], for $0 < k < 1$, any $u_0 \in L^2(\Omega_0)$, $u_1 \in H^{-1}(\Omega_0)$ and $\widetilde{w}_i \in L^2(\widehat{\Sigma}_i)$, $i = 1, 2$, Equation (10) admits a unique solution in the sense of a transposition, with u belongs $C\big([0,T]; L^2(\Omega_t)\big) \cap C^1\big([0,T]; H^{-1}(\Omega_t)\big)$. Hence, the cost functionals $\widetilde{J}_2$ and $\widetilde{J}$ above, are well defined.

The *Stackelberg-Nash* is described as follows: If the leader $\widetilde{w}_1$ makes a choice, then the follower $\widetilde{w}_2$ makes also a choice, depending on $\widetilde{w}_1$, which minimizes the cost $\widetilde{J}_2$, that is,

$$\widetilde{J}_2(\widetilde{w}_1, \widetilde{w}_2) = \inf_{\widehat{w}_2 \in L^2(\widehat{\Sigma}_2)} \widetilde{J}_2(\widetilde{w}_1, \widehat{w}_2). \tag{13}$$

4. Optimality systems The main goal in this section is to presents the optimality systems for the leader and follower controls. Initially, we consider

$\mathcal{U}_{ad} = \{(u, \widetilde{w}_2) \in L^2(Q) \times L^2(\widehat{\Sigma}_2);\ u \text{ solution of } (10)\}$, and $\widetilde{J}_2 : \mathcal{U}_{ad} \longrightarrow \mathbb{R}$ defined by (11). It is easy see that $\mathcal{U}_{ad}$ is a nonempty closed convex subset of $L^2(Q) \times L^2(\Sigma_2)$, and $\widetilde{J}_2$ is weakly coercive, weakly sequentially lower semicontinuous and strictly convex. Therefore, there exists a unique solution $\widetilde{w}_2 = \mathfrak{F}(\widetilde{w}_1)$ of problem

$$\inf_{\widetilde{w}_2 \in L^2(\widehat{\Sigma}_2)} \widetilde{J}_2(\widetilde{w}_1, \widetilde{w}_2). \tag{14}$$

After a short computation of the Gateaux derivative of the functional (11), we obtain the Euler - Lagrange equation for problem (14) given by

$$\int_0^T \int_{\Omega_t} (u - u_2)\widehat{u}\,dxdt + \sigma \int_{\widehat{\Sigma}_2} \widetilde{w}_2 \widehat{w}_2 d\,\widehat{\Sigma} = 0, \quad \forall\, \widehat{w}_2 \in L^2(\widehat{\Sigma}_2), \tag{15}$$

where $\widehat{u}$ is solution of the following system

$$\begin{cases} \widehat{u}_{tt} - \widehat{u}_{xx} = 0 \quad \text{in} \quad \widehat{Q}, \\ \widehat{u}\Big|_{\widehat{\Sigma}_1} = 0, \quad \widehat{u}\Big|_{\widehat{\Sigma}_2} = \widehat{w}_2 \quad \text{and} \quad \widehat{u}\Big|_{(\widehat{\Sigma}_1 \cup \widehat{\Sigma}_2)} = 0 \\ \widehat{u}(x, 0) = 0, \ \widehat{u}_t(x, 0) = 0, \quad x \in \Omega_0. \end{cases} \tag{16}$$

In view (15), it is very natural to introduce the adjoint state defined by

$$\begin{cases} p_{tt} - p_{xx} = u - u_2 \quad \text{in} \quad \widehat{Q}, \\ p(T) = p_t(T) = 0, \quad x \in \Omega_{\{t=T\}}, \\ p = 0 \quad \text{on} \quad \widehat{\Sigma}. \end{cases} \tag{17}$$

Multiplying (17) by $\widehat{u}$ and integrating by parts, then from (15) we deduce a characterization for follower control as follows:

$$\widetilde{w}_2 = \mathfrak{F}(\widetilde{w}_1) = \frac{1}{\widetilde{\sigma}}\, p_x \quad \text{on} \quad \widehat{\Sigma}_2. \tag{18}$$

From (16), (17) and (18), we consider the *optimality system for follower control* given by:

$$\begin{cases} u_{tt} - u_{xx} = 0 \quad \text{in} \quad \widehat{Q}, \\ p_{tt} - p_{xx} = u - u_2 \quad \text{in} \quad \widehat{Q}, \\ u\Big|_{\widehat{\Sigma}_1} = \widetilde{w}_1, \quad u\Big|_{\widehat{\Sigma}_2} = \dfrac{1}{\widetilde{\sigma}}\, p_x \quad \text{and} \quad u\Big|_{\widehat{\Sigma} \setminus \widehat{\Sigma}_0} = 0, \\ p = 0 \quad \text{on} \quad \widehat{\Sigma}, \\ u(0) = u_t(0) = 0, \quad x \in \Omega_0, \\ p(T) = p_t(T) = 0, \quad x \in \Omega_{\{t=T\}}. \end{cases} \tag{19}$$

Now, following the Stackelberg-Nash strategy, the leader $\widetilde{w}_1$ wants that the solutions u and u', evaluated at time $t = T$, to be as close as possible to $\{u^0, u^1\} \in L^2(\Omega_T) \times H^{-1}(\Omega_T)$. This will be possible if the system (19) is approximately controllable.

For this, as in [10], we assume that

$$T > \frac{e^{\frac{2k(1+k)}{(1-k)^3}} - 1}{k} \tag{20}$$

and

$$0 < k < 1. \tag{21}$$

Remark 4.1 In the literature there are several works that approach the time T given in (20) and the speed of the moving endpoint k as in (21); for more details see for example [5, 32]. In the case of $k = 1$, some results have been obtained in [4]. However, we do not extend the approach developed in this paper to the case $k = 1$. On the other hand, in the case $k > 1$, the moving boundary is a spacelike surface, on which an initial condition rather than a boundary condition needs to be imposed. For interested readers on this subject, we cite for instance [4], [3], and [32].

The next result concerns the approximate controllability with respect to the leader control. More precisely, we have the following result:

Theorem 4.2 *Assume that (20) and (21) hold. Let us consider $\widetilde{w}_1 \in L^2(\widehat{\Sigma}_1)$ and $\widetilde{w}_2$ a Nash equilibrium in the sense (13). Then*

$$\big(u(T), u'(T)\big) = \big(u(., T, \widetilde{w}_1, \widetilde{w}_2), u'(., T, \widetilde{w}_1, \widetilde{w}_2)\big) ,$$

where u solves the system (19), generates a dense subset of $L^2(\Omega_T) \times H^{-1}(\Omega_T)$.

The proof of this theorem is by well known is a direct consequence of Holmgren's Uniqueness Theorem (cf. [19]) and multiplier method. For additional discussions see Theorem 4.1 of [10].

Remark 4.3 As can be seen in [10], the income statement above is done using the decomposition of the solutions in (19)

$$(u, p) = (u_p + g, p_p + q), \tag{22}$$

where u_p, p_p, g and q are particular solutions for this system. New systems for g and q are obtained, and the author consider the following "adjoint systems" for g and q respectively:

$$\begin{cases} \varphi_{tt} - \varphi_{xx} = \psi \ \text{ in } \ \widehat{Q}, \\ \varphi = 0 \ \text{ on } \ \widehat{\Sigma}, \\ \varphi(T) = 0, \ \varphi_t(T) = 0, \ \ x \in \Omega_{\{t=T\}}, \end{cases} \tag{23}$$

and

$$\begin{cases} \psi_{tt} - \psi_{xx} = 0 \ \text{ in } \ \widehat{Q}, \\ \psi\Big|_{\widehat{\Sigma}_1} = 0, \quad \psi\Big|_{\widehat{\Sigma}_2} = \dfrac{1}{\sigma}\,\varphi_x \quad \text{and} \quad \psi\Big|_{\widehat{\Sigma}\backslash\widehat{\Sigma}_0} = 0, \\ \psi(0) = \psi_t(0) = 0, \ \ x \in \Omega_0. \end{cases} \tag{24}$$

Finally, with the previous result in hand, we can to deduce an *optimality system for leader control.* The result is the following one.

THEOREM 4.4 *Assume the hypotheses (9), (20) and (21) are satisfied. Then for* $\{f^0, f^1\}$ *in* $H_0^1(\Omega_T) \times L^2(\Omega_T)$ *we uniquely define* $\{\varphi, \psi, u, p\}$ *by*

$$\begin{cases} \varphi_{tt} - \varphi_{xx} = \psi \ \ \textit{in} \ \ \widehat{Q}, \\ \psi_{tt} - \psi_{xx} = 0 \ \ \textit{in} \ \ \widehat{Q}, \\ u_{tt} - u_{xx} = 0 \ \ \textit{in} \ \ \widehat{Q}, \\ p_{tt} - p_{xx} = u - u_2 \ \ \textit{in} \ \ \widehat{Q}, \\ \varphi = 0 \quad \textit{on} \quad \widehat{\Sigma}, \\ \psi\Big|_{\widehat{\Sigma}_1} = 0, \quad \psi\Big|_{\widehat{\Sigma}_2} = \dfrac{1}{\sigma}\,\varphi_x \quad \textit{and} \quad \psi\Big|_{\widehat{\Sigma}\backslash\widehat{\Sigma}_0} = 0, \\ \\ u\Big|_{\widehat{\Sigma}_1} = -\varphi_x, \quad u\Big|_{\widehat{\Sigma}_2} = \dfrac{1}{\sigma}\,p_x \quad \textit{and} \quad u\Big|_{\widehat{\Sigma}\backslash\widehat{\Sigma}_0} = 0, \\ p = 0 \quad \textit{on} \quad \widehat{\Sigma}, \\ \varphi(.,T) = 0, \, \varphi_t(.,T) = 0 \ \ \textit{in} \ \ \Omega_{\{t=T\}}, \\ u(0) = u_t(0) = 0 \ \ \textit{in} \ \ \Omega_0, \\ \psi(0) = \psi_t(0) = 0 \ \ \textit{in} \ \ \Omega_0, \\ p(T) = p_t(T) = 0 \ \ \textit{in} \ \ \Omega_{\{t=T\}}. \end{cases} \tag{25}$$

The optimal leader is given by

$$\widetilde{w}_1 = -\varphi_x \quad \textit{on} \ \ \widehat{\Sigma}_1,$$

where φ *corresponds to the solution of first equation in the system (25).*

The proof of this theorem is based on an argument duality due to Fenchel and Rockafellar [31] (for more details see Theorem 5.1 of [10]).

5. Main results, complete discretization and algorithm

In this section, we employ a methodology combining finite differences for the time discretization, finite elements for the space approximation, and a fixed point algorithm for the iterative solution of the discrete control problem for (25), using ideas similar to those developed in [2], [8] and [29].

Initially, introduce the notation

$$V_i := \left\{ \widetilde{w}_i \in L^2(\widehat{\Sigma}_i) \;\middle|\; i = 1, 2 \right\} \text{ and } V = V_1 \times V_2 \,,$$

where $V := L^2(\widehat{\Sigma}_0)$.

As consequence of anterior results we have that: for all $\sigma > 0$ (sufficiently large), exists an unique equilibrium $(\tilde{w}_1, \tilde{w}_2) \in V$ for the functionals $\tilde{J}_1$ and $\tilde{J}_2$, satisfying the Theorem 4.4. We can reduce (25) to a finite-dimensional problem via FEM, discretizing the problem in time and space. With this, we will seek approximate solutions u_h^{n+1} and controls $\left(\widetilde{w}_1^{n+1}, \widetilde{w}_2^{n+1}\right)$ in the approximate domain $\widehat{Q}_h^M$ (to $\widehat{Q}$) described below.

5.1. Approximation in time

We consider temporal discretization for $[0, T]$, with the time step defined by $\Delta t := T/M$, where M is a large positive integer. Then, if we set $t^m := m\Delta t$, we have

$$0 < t^1 < t^2 < \cdots < t^M = T.$$

Now, we denote the time approximation for control spaces V_1 and V_2 respectively by

$$V_1^{\Delta t} := L^2(\widehat{\Sigma}_1)^M \qquad \text{and} \qquad V_2^{\Delta t} := L^2(\widehat{\Sigma}_2)^M \,,$$

and for state space W, by:

$$W^{\Delta t} \;\text{ or }\; W^M.$$

Accordingly, we can interpret the elements of $V_i^{\Delta t}$ as controls in V_i that are piecewise constant in time.

5.2. Approximation in space

Remember that for each $t \in [0, T]$, Ω_t is a subdomain of $\mathbb{R}$, $\widehat{Q} := \Omega_t \times [0, T]$, the boundary $\widehat{\Sigma} := \widehat{\Sigma}_1 \cup \widehat{\Sigma}_2$, and the controls (in the restrictions of their domains) indicated by $\tilde{w}_1\Big|_{\widehat{\Sigma}_1}$ and $\tilde{w}_2\Big|_{\widehat{\Sigma}_2}$.

Consider $\mathcal{T}_h$ the triangulation of the domain $\widehat{Q}$. Denote by $\widehat{Q}_h$ a discretization for $\widehat{Q}$, where h is the maximum size of the edges of the triangles, with $\widehat{Q}_h$ represented by

$$\widehat{Q}_h = \bigcup\nolimits_{T_K \in \mathcal{T}_h} T_K.$$

As $\widehat{Q}$ is a polygonal region, $\widehat{Q}_h = \widehat{Q}$. In Fig. 2 below, we present the mesh generated using the Freefem++ software (v. [20]). The boundary domain must be described analytically as a parameterization. To generate the mesh, the number of points on the edge $\widehat{\Sigma}$ is considered, then the software adds internal points by subdividing the edges, generating the process of creating the triangulation, based on the Delaunay-Voronoi algorithm. Triangulation accuracy is controlled by the size of the closest boundary edges.

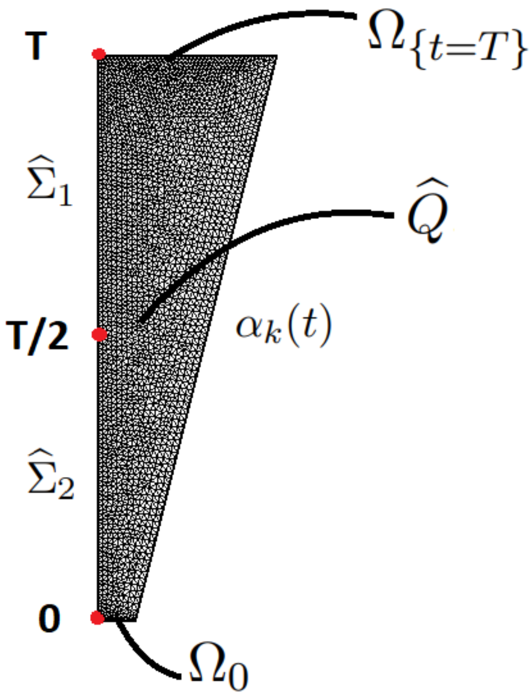

Figure 2: The domain $\widehat{Q} = \widehat{Q}_h^M$. As we modify the values of final time T, the $\widehat{Q}_h^M$ domain and its entire triangular structure are updated, thus obtaining new meshes in the finite element discretization. Further on, we present in Figures 6-8 different $\widehat{Q}_h^M$ domains.

Thus, the solution spaces

$$W = \left\{ w \in L^\infty(0,T;H_0^1(\Omega_t)) \ : \ w_t \in L^\infty(0,T;L^2(\Omega_t)) \right\}$$

can be discretized in time and space, for the construction of approximate solutions via finite elements, which will be given by $W_h^{\Delta t}$, where

$$W_h^{\Delta t} := (W_h)^M, \qquad W_h := \left\{ z \in \mathcal{C}^0(\Omega_t) \ : \ z\Big|_K \in \mathbb{P}_1(K) \ \forall K \in \mathcal{T}_h \right\}$$

with

$$W_{h,0}^{\Delta t} = (W_{h,0})^N, \qquad W_{h,0} = \left\{ z \in W_h : z\Big|_\Sigma = 0 \right\},$$

and $\mathbb{P}_1(K)$ the space of polynomial functions (piecewise linear continuous finite element) of degree ≤ 1. The $\dim(W_h) = N_h$, where N_h is the number

of vertices of $\mathcal{T}_h$.
Similarly, an approximation for the control spaces $V_i^{\Delta t}$ discretized in time and space will be given by $V_{i,h}^{\Delta t}$, defined as follows:

$$V_{i,h}^{\Delta t} = (V_{i,h})^M, \quad V_{i,h} := \left\{ z \in \mathcal{C}^0(\widehat{\Sigma}_i) \; : \; z\Big|_K \in \mathbb{P}_1(K) \;\; \forall K \in \widehat{\Sigma}_i \right\};$$

then, we set $V_h^{\Delta t} := V_{1,h}^{\Delta t} \times V_{2,h}^{\Delta t}$.

In (25) the state equation (in u and ψ) and the adjoint systems (in p and φ) can be approximated in time and space incorporating (for instance) implicit Euler finite differences in time and spatial P_1-Lagrange finite element techniques. That allows us to compute a state $u_h^{\Delta t}$ and two adjoint states $p_h^{\Delta t}$ and $\varphi_h^{\Delta t}$ for each control pair $\widetilde{w} = (\widetilde{w}_1, \widetilde{w}_2) \in V_h^{\Delta t}$.

In accordance with those definitions, we can approximate the problem to obtain a pair control $(\widetilde{w}_1,\, \widetilde{w}_2) \in V$ by a finite dimensional problem:

$$\begin{cases} \dfrac{\partial \widetilde{J}_{1,h}^{\Delta t}}{\partial \widetilde{w}_1}(\widetilde{w}_1, \widetilde{w}_2) = 0, \\ \\ \dfrac{\partial \widetilde{J}_{2,h}^{\Delta t}}{\partial \widetilde{w}_2}(\widetilde{w}_1, \widetilde{w}_2) = 0, \end{cases} \tag{26}$$

where the $\widetilde{J}_{i,h}^{\Delta t}$ are the finite-dimensional versions of the $\widetilde{J}_i$ induced by time and space approximations.

5.3. Fixed–Point Method for the Discretized Problem

To model the problem using Freefem++, one must know the variational formulation for the problem. As we will use an iteration process in time, we will present the algorithm for the approximate problem already considering its variational formulation and its total discretization. Now, we can solve the approximate formulation (26) for a the equivalent problem using the fixed–point algorithm as follows:

ALGORITHM:

a) Choose $\widetilde{w}_0 := (\widetilde{w}_{1,0},\, \widetilde{w}_{2,0}) \in V_h^{\Delta t}$ (where $\widetilde{w}_{i,0} := \widetilde{w}_i(0) \in V_{i,h}^{\Delta t}$) and introduce an approximation $u_{0,h} \in W_{h,0}$ to u_0.

b) Then, for given $n \geq 0$, compute the approximate state u_h^n by solving

$$\begin{cases} u_h^{n,0} = u_{h,0}\,, \quad u_h^{n,1} = u_h^{n,0} + (\Delta t) \cdot u_{h,1}\;, \\ \displaystyle\int_{\Omega_t} \left(\frac{1}{(\Delta t)^2} (u_h^{n,m+1} - 2u_h^{n,m} + u_h^{n,m-1}) z + \nabla u_h^{n,m+1} \cdot \nabla z \right) dx = 0\,, \\ \forall z \in W_{h,0}, \quad u_h^{n,m+1} \in W_{h,0}, \quad m = 1, ..., M-1, \end{cases} \tag{27}$$

and assuming that $u_h^{n,m}$ and $u_2(x,t^m)$ are known, compute the approximate adjoint states $p_h^{n,m}$ (for $u_h^{n,m}$), by solving

$$\begin{cases} p_h^{n,M} = 0\ , \quad p_h^{n,M-1} = 0 \\ \displaystyle\int_{\Omega_t}\left(\frac{1}{(\Delta t)^2}(p_h^{n,m+1} - 2p_h^{n,m} + p_h^{n,m-1})z + \nabla p_h^{n,m-1}\cdot\nabla z\right)dx \\ \displaystyle = \int_{\Omega_t}(u_h^{n,m-1} - u_2(x,t^{m-1}))\cdot z\,dx \\ \forall z \in W_{h,0},\ \ p_h^{n,m} \in W_{h,0},\ \ m = M-1,\ M-2,\ \dots,\ 1 \end{cases} \tag{28}$$

c) Now, for given $n \geq 0$ consider known $\left(\psi_h^n(0),\ \psi_{1,h}^n(0)\right) \in W_{h,0}^{\Delta t} \times W_{h,0}^{\Delta t}$ an approximation to $(\psi(0),\ \psi'(0)) \in W \times W$, and compute the approximate state ψ_h^n to ψ, solving

$$\begin{cases} \psi_h^{n,0} = \psi_h^{1,0} = 0\,, \quad \psi_h^{n,1} = \psi_h^{n,0} + (\Delta t)\cdot\psi_{h,1}\ , \\ \displaystyle\int_{\Omega_t}\left(\frac{1}{(\Delta t)^2}(\psi_h^{n,m+1} - 2\psi_h^{n,m} + \psi_h^{n,m-1})z + \nabla\psi_h^{n,m+1}\cdot\nabla z\right)dx = 0\,, \\ \forall z \in W_{h,0},\ \ \psi_h^{n,m+1} \in W_{h,0},\ \ m = 1, \dots, M-1, \end{cases} \tag{29}$$

in addition compute the approximate adjoint states $\varphi_h^{n,m}$, with $m = M-1,\ M-2,\ \dots,\ 1$ (where $\varphi_h^{n,M}$ and $\varphi_h^{n,M-1}$ are known), by

$$\begin{cases} \varphi_h^{n,M} = 0\ , \quad \varphi_h^{n,M-1} = 0 \\ \displaystyle\int_{\Omega_t}\left(\frac{1}{(\Delta t)^2}(\varphi_h^{n,m+1} - 2\varphi_h^{n,m} + \varphi_h^{n,m-1})z + \nabla\varphi_h^{n,m-1}\cdot\nabla z\right)dx \\ \displaystyle = \int_{\Omega_t}\psi_h^{n,m-1}\cdot z\,dx \\ \forall z \in W_{h,0},\ \ \varphi_h^{n,m} \in W_{h,0},\ \ m = M-1,\ M-2,\ \dots,\ 1 \end{cases} \tag{30}$$

and, finally, compute

$$\widetilde{w}_1^{n+1} = -\varphi_x^n\Big|_{\hat{\Sigma}_1} \tag{31}$$

and

$$\widetilde{w}_2^{n+1} = \frac{1}{\sigma}p_x^n\Big|_{\hat{\Sigma}_2}, \tag{32}$$

with σ-fixed.

6. Illustrative Numerical Examples Thanks to the results obtained in the anterior sections and theoretical results obtained in [10], we can consider for each $\widetilde{w}_1$, the *Nash equilibrium* $\widetilde{w}_2$ associated to solution u of (10). The computations have been performed using Free*fem*++, which is a high-performance free software designed to solve problems of PDEs (v. [20])[1]. The results of numerical calculation are presented in the table 1, 2 and the table 3. The graphic representations are obtained in combination with MatLab and they are presented in the figures 8-5. For all experiments the number of time steps in $M = 100$ (that gives $\Delta t = T/M$). We consider $u_2 = 10$ fixed, the initial conditions $u\Big|_{\Omega_0}$ are given by $u(0) = 0$ and $u'(0) = 0$. All initial and boundary conditions were programmed considering the information provided in the system (25).

We consider the interval $\widehat{\Sigma}_0 = (0, T)$ as control domain, where $\widehat{\Sigma}_1 = (T/2, T)$ and $\widehat{\Sigma}_2 = (0, T/2)$. As the time for the problem must satisfy (20), with k defined by (21), we define T_c as time of control (with $T > T_c$) and k are fixed by

$$T_c = \frac{e^{\frac{2k(1+k)}{(1-k)^3}}}{k} \quad \text{and} \quad k = \frac{1}{4}.$$

Now, we present several tests for the algorithms in the section (5.3). Considering $\varepsilon = 10^{-5}$ and the stopping criterion is determined by:

$$\frac{\|(\widetilde{w}_1^{n+1}, \widetilde{w}_2^{n+1}) - (\widetilde{w}_1^{n}, \widetilde{w}_2^{n})\|}{\|(\widetilde{w}_1^{n+1}, \widetilde{w}_2^{n+1})\|} \leq \varepsilon.$$

7. Conclusions We present a numerical and computational approach for the hierarchical control problem of the wave equation, considering the moving boundary and the controls that act on a piece of the boundary. A combination of the Finite Element and the Finite Difference Method is used to build approximate solutions to the time-dependent problem, adding a fixed point algorithm to evaluate the computational convergence of the results obtained during the evolution process. With this, we established the feasibility of simulating the problems in which hierarchical control acts on the mobile border. We use the proven results in [10] to ensure the validity of the results that support the numerical part developed.

8. Additional comments

The same ideas and techniques can be adapted and applied to the computation of equilibrium problems and hierarchical control in many recent other situations: In [6], numerical results are presented in Nash equilibria for problems in dimension 3; in [1] null controllability for hierarchical problems with

[1] As its name implies, it is a free software based on the Finite Element Method (more details are available at https://freefem.org/).

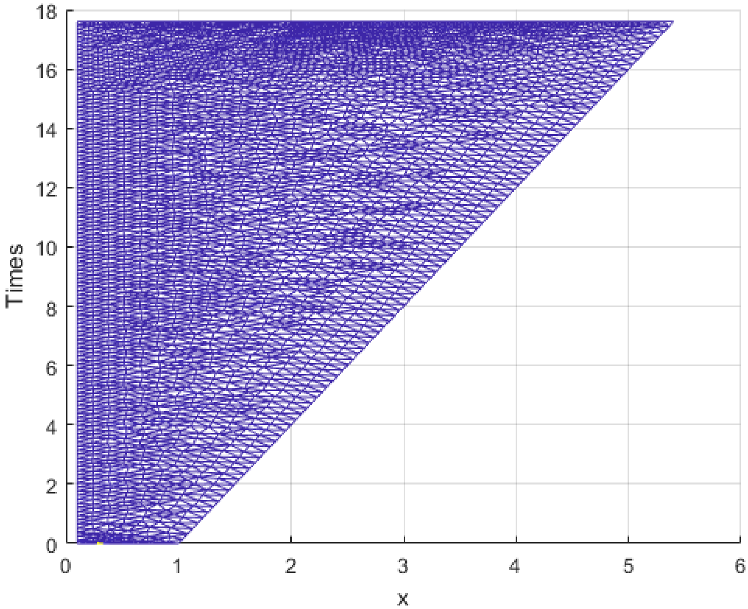

Figure 3: Domain for $k = 1/4$ and $T = 2T_c$. Nb of vertices = 2916, Nb of triangles = 5526, Border length = 41.936 .

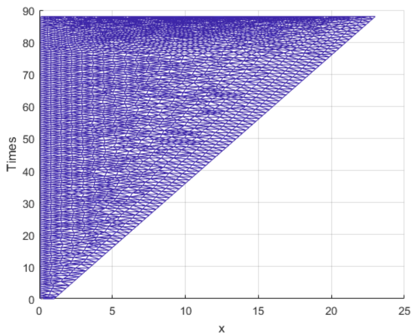

Figure 4: Domain for $k = 1/4$ and $T = 5T_c$. Nb of vertices = 2319, Nb of triangles = 4332, Border length = 202.484 .

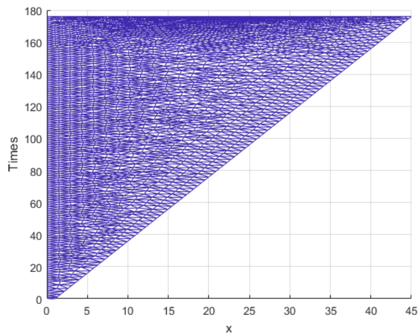

Figure 5: Domain for $k = 1/4$ and $T = 10T_c$. Nb of vertices = 2236, Nb of triangles = 4166, , Border length = 403.167 .

dynamic boundary; for hierarchical control in problems with a moving boundary (see [24], [11] and [9]); hierarchic control for parabolic systems (see [21], [23] and [22]) and Nash equilibria in single-objective optimization problems (see [28]). It can also be extended into similar analyses for other types of hierarchical control problems, such as *Stokes, Navier-Stokes, Schrödinger* (in [17] some results are presented to Navier-Stokes equations and [18] to Schrödinger

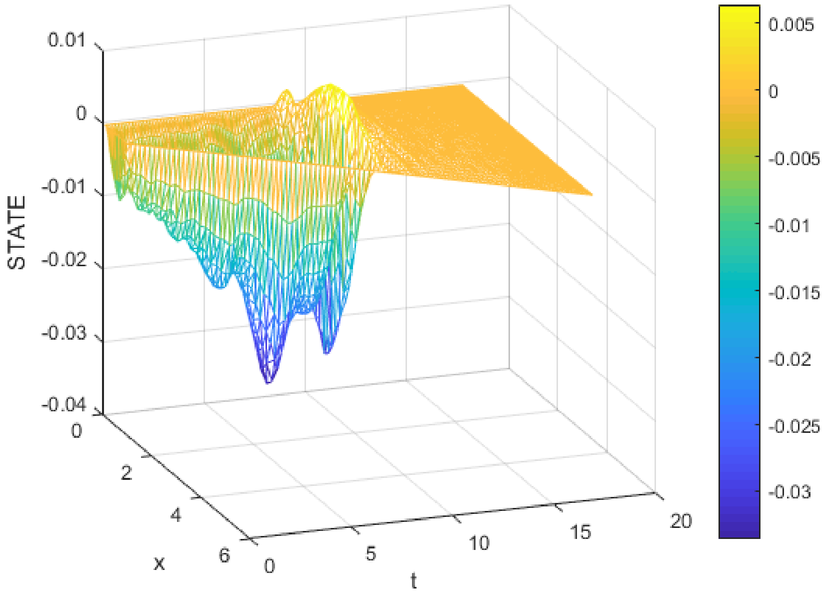

Figure 6: Final state for the approximate solution u^n in the time $T = T_c$. Iterates to the stopping criterion: 6.

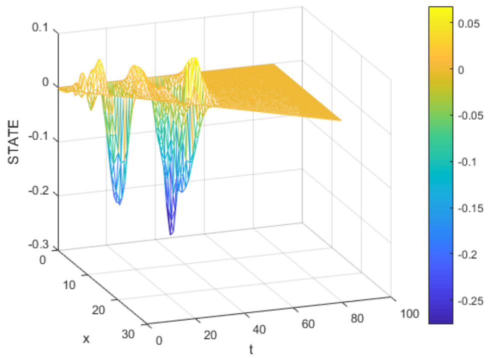

Figure 7: Final state for the approximate solution u^n in the time $T = 5 \cdot T_c$. Iterates to the stopping criterion: 7.

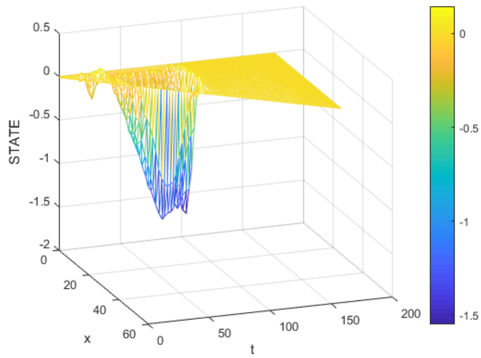

Figure 8: Final state for the approximate solution u^n in the time $T = 10T_c$. Iterates to the stopping criterion: 8.

Final states with change $T = T_c, 2 \cdot T_c, \ldots, 10 \cdot T_c$, fixed $u_2 = 10$ and $\sigma = 10^2$. The maximum number of iterates = 100.

equation).

Acknowledgments: This work was supported by Universidade Estadual do Piauí, SIGPROP-UESPI Project N^o 0646/2021 and EDITAL FAPEPI/ MCT/ CNPq N^o 007/2018: Researchers Young Infrastructure Program - Projects First Programs. Isaías Pereira de Jesus

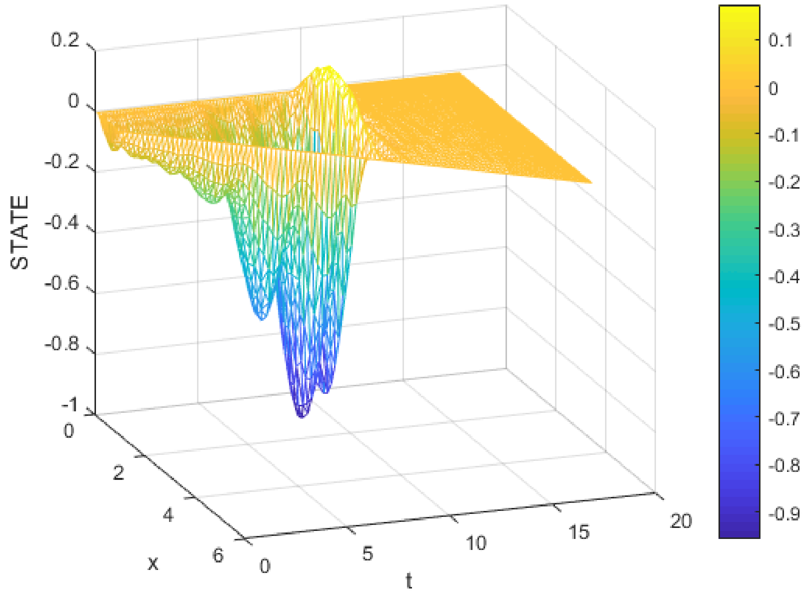

Figure 9: The number of iterations needed for convergence criterion when $\sigma = 10, 10^2, ..., 10^{10}$.

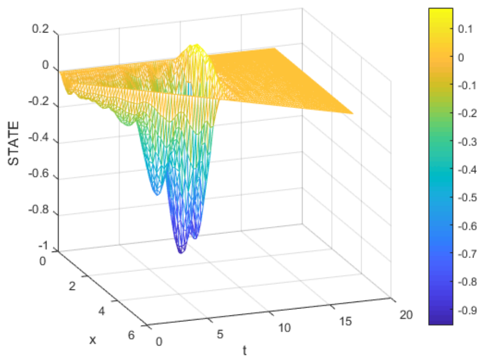

Figure 10: Final state in $T = T_c$ and $\sigma = 10$.

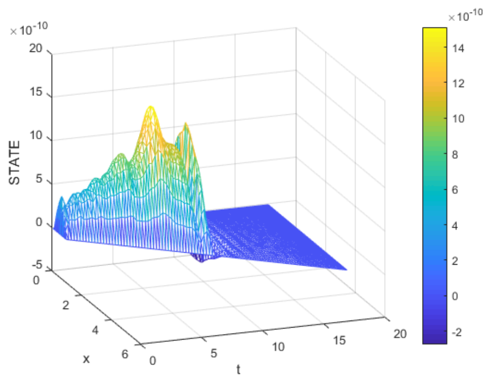

Figure 11: Final state in $T = T_c$ and $\sigma = 10^{10}$.

was partially supported by grants from CNPq/Brazil [Grant: 307488/2019-5].

A. Tables

Time	$\|u-u^n\|_{L^2(\hat{Q})} < \varepsilon$	$\sum_{i=1}^{2} \|\tilde{w}_i - \tilde{w}_i^n\|_{L^2(\hat{\Sigma})} < \varepsilon$	Iterates
T_c	$4.23731 \cdot 10^{-6}$	$8.94841 \cdot 10^{-8}$	6
$2 \cdot T_c$	$1.39288 \cdot 10^{-5}$	$6.04906 \cdot 10^{-6}$	7
$3 \cdot T_c$	$5.38065 \cdot 10^{-5}$	$3.47866 \cdot 10^{-7}$	7
$4 \cdot T_c$	$9.46165 \cdot 10^{-5}$	$7.61072 \cdot 10^{-7}$	7
$5 \cdot T_c$	$9.84504 \cdot 10^{-5}$	$9.49046 \cdot 10^{-7}$	7
$6 \cdot T_c$	$2.22432 \cdot 10^{-5}$	$1.62926 \cdot 10^{-7}$	8
$7 \cdot T_c$	$8.91691 \cdot 10^{-5}$	$6.78541 \cdot 10^{-7}$	8
$8 \cdot T_c$	$2.50240 \cdot 10^{-4}$	$1.41019 \cdot 10^{-6}$	8
$9 \cdot T_c$	$4.04092 \cdot 10^{-4}$	$1.85044 \cdot 10^{-6}$	8
$10 \cdot T_c$	$5.41312 \cdot 10^{-4}$	$2.14904 \cdot 10^{-6}$	8

Table 1: Domains construction in function of time $T = T_c$. The maximum number of iterates = 100, $k = 1/4$, $\sigma = 10^2$ and $u_2 = 10$ fixed.

Time	N.° Vertices	N.° Triangles	Border Length
T_c	2916	5526	41.936
$2 \cdot T_c$	2580	4854	82.073
$3 \cdot T_c$	2411	4516	122.210
$4 \cdot T_c$	2365	4424	162.347
$5 \cdot T_c$	2319	4332	202.484
$6 \cdot T_c$	2309	4312	242.620
$7 \cdot T_c$	2316	4326	282.757
$8 \cdot T_c$	2273	4240	322.894
$9 \cdot T_c$	2246	4186	363.031
$10 \cdot T_c$	2236	4166	403.167

Table 2: Domains construction in function of time $T = T_c$. The maximum number of iterates = 100, $k = 1/4$, $\sigma = 10^2$ and $u_2 = 10$ fixed.

References

[1] I. Boutaayamou, L. Maniar, and O. Oukdach. Stackelberg-nash null controllability of heat equation with general dynamic boundary conditions. *arXiv preprint arXiv:2109.02356*, 2021. Cited on p. 119.

[2] P. P. Carvalho and E. Fernández-Cara. On the computation of nash and pareto equilibria for some bi-objective control problems. *Journal of Scientific Computing*, 78(1):246–273, 2019. Cited on pp. 108 and 114.

[3] L. Cui and H. Gao. Exact controllability for a wave equation with mixed

σ	Iterates	Error for stopping criteria
10	34	7.77814×10^{-6}
10^2	6	8.94080×10^{-6}
10^3	4	2.00607×10^{-6}
10^4	3	3.10847×10^{-6}
10^5	3	3.10853×10^{-8}
10^6	3	3.10861×10^{-10}
10^7	2	5.61446×10^{-6}
10^8	2	5.61446×10^{-7}
10^9	2	5.61446×10^{-8}
10^{10}	2	2.61444×10^{-8}

Table 3: The iterates and convergence error with change σ. The maximum number of iterates = 100, $k = 1/4$, $T = T_c$ and $u_2 = 10$ fixed.

boundary conditions in a non-cylindrical domain. *Electron. J. Differ. Equ*, 101(1), 2014. Cited on p. 113.

[4] L. Cui, X. Liu, and H. Gao. Exact controllability for a one-dimensional wave equation in non-cylindrical domains. *Journal of Mathematical Analysis and Applications*, 402(2):612–625, 2013. Cited on pp. 110 and 113.

[5] L. Cui, Y. Jiang, and Y. Wang. Exact controllability for a one-dimensional wave equation with the fixed endpoint control. *Boundary Value Problems*, 2015(1):1–10, 2015. Cited on p. 113.

[6] P. P. de Carvalho. Some numerical results for control of 3d heat equations using nash equilibrium. *Computational and Applied Mathematics*, 40(3): 1–30, 2021. Cited on p. 119.

[7] P. P. de Carvalho and E. Fernández-Cara. Numerical stackelberg–nash control for the heat equation. *SIAM Journal on Scientific Computing*, 42(5):A2678–A2700, 2020. Cited on p. 108.

[8] P. P. de Carvalho, E. Fernández-Cara, and J. B. L. Ferrel. On the computation of nash and pareto equilibria for some bi-objective control problems for the wave equation. *Advances in Computational Mathematics*, 46(5):1–30, 2020. Cited on pp. 108 and 114.

[9] I. P. de Jesus. Hierarchical control for the wave equation with a moving boundary. *Journal of Optimization Theory and Applications*, 171(1): 336–350, 2016. Cited on p. 120.

[10] I. P. de Jesus. Approximate controllability for a one-dimensional wave equation with the fixed endpoint control. *Journal of Differential Equations*, 263(9):5175–5188, 2017. Cited on pp. 108, 110, 113, 114, and 119.

[11] I. P. de Jesus and S. B. de Menezes. On the approximate controllability of stackelberg–nash strategies for linear heat equations in $mathbbR^n$ with potentials. *Applicable Analysis*, 94(4):780–799, 2015. Cited on p. 120.

[12] O. P. de Sá Neto and H. A. S. Costa. Estimation of decoherence in electromechanical circuits. *Phys. Lett., A*, 383(31):4, 2019. ISSN 0375-9601. doi: 10.1016/j.physleta.2019.125875. Id/No 125875; Zbl 1477.81141. Cited on p. 108.

[13] O. P. de Sá Neto and M. C. de Oliveira. Quantum bit encoding and information processing with field superposition states in a circuit. *Journal of Physics B: Atomic, Molecular and Optical Physics*, 45(18):185505, sep 2012. doi: 10.1088/0953-4075/45/18/185505. Cited on p. 108.

[14] O. P. de Sá Neto, M. C. de Oliveira, and A. O. Caldeira. Generation of superposition states and charge-qubit relaxation probing in a circuit. *Journal of Physics B: Atomic, Molecular and Optical Physics*, 44(13): 135503, jun 2011. doi: 10.1088/0953-4075/44/13/135503. Cited on p. 108.

[15] O. P. de Sá Neto, M. C. de Oliveira, F. Nicacio, and G. J. Milburn. Capacitive coupling of two transmission line resonators mediated by the phonon number of a nanoelectromechanical oscillator. *Phys. Rev. A*, 90: 023843, Aug 2014. doi: 10.1103/PhysRevA.90.023843. Cited on p. 108.

[16] O. P. de Sá Neto, M. C. de Oliveira, and G. J. Milburn. Temperature measurement and phonon number statistics of a nanoelectromechanical resonator. *New Journal of Physics*, 17(9):093010, 2015. doi: 10.1088/1367-2630/17/9/093010. Cited on p. 108.

[17] E. Fernández-Cara and I. Marín-Gayte. Theoretical and numerical results for some bi-objective optimal control problems. *Commun. Pure Appl. Anal.*, 19(4):2101–2126, 2020. ISSN 1534-0392. doi: 10.3934/cpaa.2020093. Zbl 1437.35534. Cited on p. 120.

[18] D. C. Gomes, M. A. Rincon, M. D. G. d. Silva, and G. O. Antunes. Theoretical and computational analysis of a nonlinear schrödinger problem with moving boundary. *Advances in Computational Mathematics*, 45(2): 981–1004, 2019. Cited on p. 120.

[19] P. H Müller. L. hörmander, linear partial differential operators. viii+ 284 s. m. 1 fig. berlin/göttingen/heidelberg 1963. springer-verlag. preis geb. dm 42,-. *Zeitschrift Angewandte Mathematik und Mechanik*, 44(3): 139–139, 1964. Cited on p. 113.

[20] F. Hecht. New development in freefem++. *J. Numer. Math.*, 20(3-4): 251–265, 2012. ISSN 1570-2820. doi: 10.1515/jnum-2012-0013. URL `https://freefem.org/`. MR 3043640. Cited on pp. 115 and 119.

[21] V. Hernández-Santamaría and L. de Teresa. Robust stackelberg controllability for linear and semilinear heat equations. *Evolution Equations & Control Theory*, 7(2):247, 2018. Cited on p. 120.

[22] V. Hernández-Santamaría and L. d. Teresa. Some remarks on the hierarchic control for coupled parabolic pdes. In *Recent advances in PDEs: analysis, numerics and control*, pages 117–137. Springer, 2018. Cited on p. 120.

[23] V. Hernandez-Santamaria, L. de Teresa, and A. Poznyak. Hierarchic control for a coupled parabolic system. *Portugaliae Mathematica*, 73(2): 115–137, 2016. Cited on p. 120.

[24] J. Limaco, H. Clark, and L. Medeiros. Remarks on hierarchic control. *Journal of mathematical analysis and applications*, 359(1):368–383, 2009. Cited on p. 120.

[25] M. M. Miranda. Hum and the wave equation with variable coefficients. *Asymptotic Analysis*, 11(4):317–341, 1995. Cited on p. 111.

[26] J. Nash. Non-cooperative games. *Annals of mathematics*, pages 286–295, 1951. Cited on p. 108.

[27] D. M. Pozar. *Microwave engineering*. John wiley & sons, 2011. Cited on p. 108.

[28] A. M. Ramos. Nash equilibria strategies and equivalent single-objective optimization problems. the case of linear partial differential equations. *arXiv preprint arXiv:1908.11858*, 2019. Cited on p. 120.

[29] A. M. Ramos, R. Glowinski, and J. Periaux. Nash equilibria for the multiobjective control of linear partial differential equations. *J. Optim. Theory Appl.*, 112(3):457–498, 2002. ISSN 0022-3239. doi: 10.1023/A:1017981514093. Zbl 1012.49020. Cited on pp. 108 and 114.

[30] A. M. Ramos, R. Glowinski, and J. Periaux. Pointwise control of the Burgers equation and related Nash equilibrium problems: Computational approach. *J. Optim. Theory Appl.*, 112(3):499–516, 2002. ISSN 0022-3239. doi: 10.1023/A:1017907930931. Zbl 1027.49020. Cited on p. 108.

[31] R. T. Rockafellar. *Convex analysis*, volume 28 of *Princeton Math. Ser.* Princeton University Press, Princeton, NJ, 1970. Zbl 0193.18401. Cited on p. 114.

[32] H. Sun, H. Li, and L. Lu. Exact controllability for a string equation in domains with moving boundary in one dimension. *Electron. J. Differ. Equ*, 98(1), 2015. Cited on p. 113.

[33] H. Von Stackelberg. *Marktform und gleichgewicht.* J. springer, 1934. Cited on p. 108.

O obliczeniowych zadaniach przy wyznaczaniu sterowań hierarchicznych dla jednowymiarowej linii przesyłowej

P. P. de Carvalho, I. P. de Jesus i O. P. de Sá Neto

Streszczenie W tym artykule, motywowanym problemem fizycznym, badamy pewne aspekty numeryczne i obliczeniowe problemu sterowalności hierarchicznej w jednowymiarowym równaniu falowym w domenach z ruchomą granicą. Niektóre sterowania są na brzegu i definiują strategię równowagi między nimi, biorąc pod uwagę sterowania lidera i naśladowcę. W związku z tym wprowadziliśmy koncepcję sterowań hierarchicznych w celu rozwiązania tego problemu i przyporządkowaliśmy strategię Stackelberga między tymi strategiami. Opisane tutaj metody numeryczne składają się z kombinacji następujących elementów: metoda elementów skończonych (MES) dla aproksymacji przestrzennej; metoda różnic skończonych (FDM) do dyskretyzacji czasu i algorytm stałoprzecinkowy do rozwiązania problemu całkowitego sterowania dyskretnego. Programowanie danych i symulacje komputerowe wykonujemy w FreeFem++, a dla lepszej prezentacji eksperymentów używamy Matlaba.

2020 Klasyfikacja tematyczna AMS (2010): Primary: 93B05; Secondary: 93C05, 93C25, 65N06..

Słowa kluczowe: sterowalność; strategia Stackelberga; linia długa; równania telegrafistów; symulacja numeryczna .

Pitagoras Pinheiro de Carvalho is Doctor in Mathematics from Universidade Federal Fluminense - (UFF), with a period of Sandwich Doctorate at Universidad de Sevilla (IMUS) - Spain. Master in Mathematics from the Federal University of Paraíba - (UFPB) and Bachelor in Mathematics from the Federal University of Piauí - (UFPI). He has experience in the area of Mathematical Analysis, with an emphasis on Partial Differential Equations, Control Theory, Equilibrium Problems, Numerical Analysis and Mathematical Programming. He is interested in Control Theory, Inverse Problems, Numerical Methods for ODE's and PDE's, Partial Differential Equations, Equilibrium Problems, Mathematical Programming using MatLab and Freefem ++.

Isaias Pereira de Jesus is Licentiate in Mathematics from the Federal University of Piauí (1998), Master in Mathematics from the Federal University of Ceará (2001), PhD in Mathematics from the Federal University of Ceará (2012) and Post-Doctorate in Mathematics from the Federal University of Pernambuco. (2018). He is a Permanent Member of the Graduate Program in Mathematics (Master's and Doctorate) at Universidade Federa do Piauí. He received a Research Productivity Scholarship from the Federal University of Piauí (2018-2020). He is currently an Associate Professor I-DE at the Federal University of Piauí and a CNPq Level 2 Productivity Scholar. My research interests are control problems of phenomena modeled by Partial Differential Equations, in particular, controllability of parabolic and hyperbolic systems with a reduced number of controls.

Olimpio Pereira de Sá Neto is Physics from the Federal University of Piauí (2007), master's degree (2009) and doctorate (2013) in Physics from the State University of Campinas. I am currently an Adjunct Professor 4 at the Coordination of Computer Science at the State University of Piauí-Campus Alexandre Alves de Oliveira. In this institution, in addition to the courses taught, he have developed research involving: analytical solutions of EDPs, numerical methods applied to the interaction radiation-matter, dissipative quantum effects, measurements in quantum systems, quantum circuits, parameter estimates, quantum coherence and entanglement.

Pitágoras Pinheiro de Carvalho
Universidade Estadual do Piauí(UESPI)
Coordenação de Matemática, Teresina, PI, Brazil
E-mail: pitagorascarvalho@gmail.com

Isaías Pereira de Jesus
Universidade Federal do Piauí(UFPI)
Departamento de Matemática, 64049-550, Teresina, PI, Brazil
E-mail: isaias@ufpi.edu.br

Olimpio Pereira de Sá Neto
Universidade Estadual do Piauí(UESPI)
Coordenação de Ciências da Computação, Parnaíba, PI, Brazil
E-mail: olimpioqedc@gmail.com

Communicated by: Jerzy Klamka; Łukasz Stettner

(Received: 1st of July 2022; revised: September 23, 2022)